

Fracture Toughness Measurement of Thin Films on Compliant Substrate Using Controlled Buckling Test

Zhong Chen*, Zhenghao Gan

School of Materials Science & Engineering, Nanyang Technological University, Singapore 639798

Abstract

Thin films and multilayered structures are increasingly used in the industry. One of the important mechanical properties of these thin layers is the fracture toughness, which may be quite different from the known value of the bulk sample due to microstructural difference. In the design towards device flexibility and scratch resistance, for example, fracture toughness is an important parameter of consideration. This work presents a testing scheme using controlled buckling experiment to determine the fracture toughness of brittle thin films prepared on compliant substrates. When the film is under tension, steady-state channelling cracks form in parallel to each other. Critical fracture strain can be calculated by the measuring the displacement of the buckled plate. The fracture toughness can then be obtained with the help of finite element calculation. When the substrate experiences plastic deformation, the energy release rate is increased by the degree of plasticity. Fracture toughness measurement of two types of thin film Cu-Sn intermetallic compounds has been given to illustrate the merits of such a test scheme.

Key Words: Thin film fracture; Fracture toughness; Controlled buckling test, Intermetallic compound

* Corresponding author. Fax: +65 6790 9081;
E-mail address: aszchen@ntu.edu.sg (Z. Chen)

1. Introduction

Thin films and multilayered structures are increasingly employed in all sectors of modern industry. For example in the semiconductor industry, devices and interconnect lines are fabricated by various types of thin film technologies [1]. On an optical lens, multilayers are coated for various functions such as scratch resistance, anti-reflection, etc. [2]. Liquid crystal displays and organic light emitting devices typically employ a layer of transparent conducting oxide (TCO) as an electrode. TCOs are usually made of brittle oxides, such as indium-tin oxide (ITO) [3] or indium-zinc oxide (IZO) [4]. Superhard wear-resistance coatings are frequently used in advanced engineering cutting tools and biomedical implants [5-7]. Design and reliability prediction of thin films and multilayers requires the knowledge of mechanical properties of these thin film materials. These properties include elasticity modulus, hardness, strength and fracture toughness. Elasticity modulus and hardness can be measured by nano-indentation on the thin film. In particular, the elasticity modulus of a material is insensitive to its microstructure, therefore it is possible to use the available data obtained from a bulk specimen. The fracture toughness, however, may be quite different from the value obtained from the bulk specimen since it is sensitive to the microstructure. With thin films typically of the thickness of 1 micron or less, the grain size is usually of the order of 1 micron or less. The conventional fracture specimens, on the other hand, are of the order of tens and hundreds of millimetres with the grain size at least one order higher than 1 micron.

This paper presents a testing scheme using controlled buckling experiment to measure the fracture toughness of brittle thin films on compliant substrates. When the film-on-substrate system buckles under uniaxial loading, one side is bent under tension and the other compression. The film to be tested is placed on the tension side of the bending. The work is focused on the case that the thickness of the film is much less than the substrate thickness. Under this condition, the stress/strain in the film can be treated as uniform through the film

thickness. Steady-state channelling cracks will form when a critical stress (or strain) is reached. The strain can be calculated by the displacement in the buckle. The fracture toughness can then be determined based on the measured critical fracture strain. When the substrate experiences plastic deformation, the energy release rate is shown to be affected by the degree of plasticity. The fracture toughness of two types of thin film Cu-Sn and intermetallic compounds have been measured by this approach. The results are discussed and compared with the ones by other researcher.

2. The Controlled Buckling Test

2.1. Experimental Setup

The controlled buckling test is sketched in figure 1. The ends of the composite (film on substrate) plate are either free (simple support) or clamped (built-in). In the current analysis, the film is brittle so that it can only deform elastically till the point of fracture. The substrate can either be elastic or plastic at the point of the film fracture.

The experiment is carried out with progressive displacement applied, either using a mechanical testing machine [8-11], or manually by an operator using a fixture to be observed under an optical microscope. As shown in figure 2, the two ends of the test piece (thin film coated on compliant substrate) are clamped. One clamped end is fixed while load is applied through the movable end. With the increase of load, the film that is placed on the tension side of the bend will be critically stretched to the point of cracking. The film cracking can be monitored either by the resistance change, as in the case of conducting film on insulating substrate [8-11], or by direct observation under an optical microscope [11, 12] (figure 2). The latter is suitable for all types of film and substrate combinations and is used in the current work. Once the film cracks, the test will stop. The only parameter that needs to be taken after the experiment is the lateral displacement at which the film crack starts to occur. The

corresponding strain in the film is the critical fracture strain and it can be calculated by large displacement beam bending theory. The next section will provide details for the calculation of fracture strain and the critical energy release rate for thin film fracture.

2.2 Analysis on Thin Film Fracture on Compliant Substrate

2.2.1. Elastic solution

When both the film and substrate remain elastic to the point of film fracture, the film-on-substrate plate under controlled buckling test can be analysed as a plane strain beam loaded along its axis. Large deformation buckling theory of beams correlates the maximum curvature of bending to the displacement by the following equations [13]:

$$\delta = 2 \left[1 - \frac{E(k)}{K(k)} \right]; \quad \frac{l}{R} = 4K(k)k \quad (1)$$

where $K(k)$ and $E(k)$ are complete elliptic integrals of the first and second, L the original length of the beam, R the radius of curvature, and $\delta = e/L$ the contraction ratio. k is only an intermediate variable in the above equation. For the two schemes in figure 1, $l = L$ for simple support and $l = L/2$ for built-in ends. By input of the displacement, e , measured from the experiment, the radius of bending curvature, $1/R$, can be calculated.

With the assumption that the ratio of film thickness to the substrate thickness is much less than 1, the neutral axis is close to the geometric centre of the composite beam. Thus the strain in the film, ε_f , is approximately uniform and is given by

$$\varepsilon_f = \frac{(h + h_f)}{2R} \quad (2)$$

where h and h_f are the thickness of the substrate and film respectively.

When the film is under tensile stress, channelling crack will form through the width of the plate when the critical bending strain (stress) is reached. This type of behaviour has been studied by Beuth [14], Hutchinson [15], and Hutchinson and Suo [16]. The channelling crack

is an indication of steady-state propagation of through film thickness cracks. The steady state energy release rate, G , is given by [14, 15]

$$G = \frac{1}{2} \bar{E}_f \varepsilon_f^2 \pi h_f g(\alpha, \beta) \quad (3)$$

in which \bar{E}_f is the plane strain modulus of the film. The factor $g(\alpha, \beta)$ is a function of the Dundurs' parameter, α and β , which for plane strain condition are given by

$$\alpha = \frac{\bar{E}_f - \bar{E}}{\bar{E}_f + \bar{E}}; \quad \beta = \frac{\bar{E}_f \left(\frac{1-2\nu}{1-\nu} \right) - \bar{E} \left(\frac{1-2\nu_f}{1-\nu_f} \right)}{2(\bar{E}_f + \bar{E})} \quad (4)$$

where \bar{E} is the plane strain modulus of the substrate, and ν and ν_f stand for the Poisson's ratio of the substrate and the film, respectively. Of these two parameters that determine the value of $g(\alpha, \beta)$, α is far more influential. β has nearly negligible effect on $g(\alpha, \beta)$. The finite element scheme that calculates $g(\alpha, \beta)$ has been given elsewhere [14]. The critical energy release rate, or toughness, G_{Ic} , of the film can be obtained by equation (3) once the critical fracture strain, ε_f , is known from equation (2).

2.2.2. Elastic-plastic solution

When the substrate exceeds the elastic limit, a uniaxial elastic - linear work hardening stress - strain relation for the substrate material is assumed in the current work:

$$\sigma = \begin{cases} E\varepsilon & \text{for } \varepsilon \leq \varepsilon_y \\ E\varepsilon_y + \lambda E(\varepsilon - \varepsilon_y) & \text{for } \varepsilon > \varepsilon_y \end{cases}, \quad (5)$$

where ε_y is the strain at the onset of plastic deformation, and λ the linear work-hardening coefficient. The detailed buckling analysis for an elastic - linear work hardening plate has been provided by Liu *et al* [17]. Again from the lateral displacement, e , the maximum bending curvature in the beam can be obtained. The energy release rate with substrate

yielding can still be expressed by the general form of equation (3), but the $g(\alpha, \beta)$ now becomes a function of not only α and β , but also the applied stress level (σ/σ_y) and the work-hardening coefficient (λ):

$$G = \frac{1}{2} \bar{E}_f \varepsilon_f^2 \pi h_f g\left(\alpha, \beta, \frac{\sigma}{\sigma_y}, \lambda\right) \quad (6)$$

Finite element scheme proposed by Beuth and Klingbeil [18] to calculate $g(\alpha, \beta)$ is adopted here. Commercial software package ABAQUS is used for the calculation. The film-on-substrate model consists of 8-node quadratic, reduced integration, hybrid 2-D solid elements. In Beuth and Klingbeil's work, the substrate material follow a Ramberg-Osgood constitutive relation. Ramberg-Osgood relation works well with large plasticity problems. However if the deformation is not far beyond the elastic limit, using Ramberg-Osgood relation may cause considerable error. The constitutive equation in equation (5) overcomes this deficiency by the two-stage relation. As far as thin film fracture experiment is concerned, we believe equation (5) will yield more accurate results.

2.2.3. Effect of plastic deformation on the cracking tendency

Figure 3 shows the effect of (σ/σ_y) on the value of $g\left(\alpha, \beta, \frac{\sigma}{\sigma_y}, \lambda\right)$ when $\lambda = 0.001$ and 0.05 while β is fixed at 0. The value of $g\left(\alpha, \beta, \frac{\sigma}{\sigma_y}, \lambda\right)$ increases from elastic deformation to plastic deformation at all α 's, and the higher the degree of plasticity (σ/σ_y) , the greater the g factor. Physically, yielding of the substrate at the vicinity of the running crack enhances crack opening, so that the film is more likely to crack. The increase is more pronounced when the film is much stiffer than the substrate (α is closer to unity). Comparing figures 3(a) and (b), it

is clear that when the substrate work hardens more (greater λ), the increase in $g\left(\alpha, \beta, \frac{\sigma}{\sigma_y}, \lambda\right)$

is less. For example, when $\frac{\sigma}{\sigma_y} = 5$ and $\alpha = 0.95$, $g\left(\alpha, \beta, \frac{\sigma}{\sigma_y}, \lambda\right) = 16.86$ for $\lambda = 0.001$ and

14.91 for $\lambda = 0.05$. This is because that when reaching the same stress level, the substrate deforms less with more highly work hardened material. As a result, the crack opening is

smaller. Figure 4 confirms this argument by plotting $g\left(\alpha, \beta, \frac{\sigma}{\sigma_y}, \lambda\right)$ as a function of $\frac{\sigma}{\sigma_y}$

when $\alpha = 0.95$. It is clear that with the increase of λ , the g factor approaches the elastic solution at all stress levels.

3. Results and Discussion with Cu-Sn Intermetallic Thin Films

Between Cu and Sn, there exists two types of intermetallic compound (IMC)s: Cu_6Sn_5 and Cu_3Sn . Cu-Sn IMC in thin film form was prepared on polymer substrates using DC magnetron co-sputtering [11, 12]. Cu_3Sn intermetallic thin film was formed by co-depositing Cu and Sn with atomic ratio of 3:1 on polyetherimide (Ultem) substrates. The samples were then annealed at 150°C in inert nitrogen ambience for one day. Cu_6Sn_5 intermetallic thin film was formed by co-depositing Cu and Sn with atomic ratio of 6:5 on polycarbonate substrates. Annealing was done at a lower temperature of 50°C in inert nitrogen ambience for one day. The thickness of the intermetallic films in both cases was 800 nm after trial and error with processing parameters. The stoichiometric compositions were maintained during co-deposition by controlling the deposition rates of individual targets. The average grain size for Cu_3Sn is about 100 nm, and the one for Cu_6Sn_5 ranges between 200 - 400 nm [12].

Table 1 summarizes the material's properties and thickness of the two types of Cu-Sn IMCs and the substrates used. Figure 5 shows typical channelling cracks in the IMC film under

SEM after the experiment. The critical energy release rate (or fracture toughness), G_{Ic} , was obtained from 8 - 9 samples in each type of the IMC films. The fracture toughness for the Cu_3Sn film was $65.5 \pm 8.0 \text{ J/m}^2$, and the one for Cu_6Sn_5 film was $55.9 \pm 7.3 \text{ J/m}^2$ (table 1). It is noted that the variation of the fracture toughness among samples is small compared with conventional fracture test in bulk specimens. This is due to the fact that channelling crack is a lateral propagation of a through-thickness crack. The maximum flaw size is defined by the film thickness. Therefore the cracking is less sensitive to surface flaws as in the case of bulk fracture test.

In order to compare with other reported results on Cu-Sn intermetallic compound fracture, G_{Ic} is converted to another fracture toughness parameter, K_{Ic} , the critical stress intensity factor. Taking the Young's modulus and Poisson's ratio for Cu_3Sn and Cu_6Sn_5 in table 1 from reference [19], individual G_{Ic} value is converted to K_{Ic} first, then its average and standard deviation are calculated. The average K_{Ic} is $2.83 \text{ MPa}\cdot\text{m}^{1/2}$ for the Cu_3Sn with a standard deviation of $0.16 \text{ MPa}\cdot\text{m}^{1/2}$ (table 1). For Cu_6Sn_5 films, $K_{Ic} = 2.36 \pm 0.15 \text{ MPa}\cdot\text{m}^{1/2}$. The K_{Ic} for Cu_6Sn_5 is quite close to the reported $2.73 \pm 0.63 \text{ MPa}\cdot\text{m}^{1/2}$ by Ghosh [20], where indentation method was used on annealed cast ingot. Our K_{Ic} value for Cu_3Sn is much lower than the $5.72 \pm 0.86 \text{ MPa}\cdot\text{m}^{1/2}$ by Ghosh [20] but closer to the $2.1 \pm 0.8 \text{ MPa}\cdot\text{m}^{1/2}$ reported by Hoyt (see table III in reference [20]). Factors that may influence the fracture toughness include microstructure, lattice orientation, and even test method. Indentation measurement for fracture toughness is a semi-empirical approach. Even if it does yield reasonably accurate results, there is still another clear difference between our specimens and the one in Ghosh's work, which is the grain size. The grain size for Cu_3Sn films in our work is well below $1 \mu\text{m}$, while the one in Ghosh's work is $72 \mu\text{m}$ or above. As a result, indentation cracking was always within an individual grain and the measurement may be affected by the crystal orientation. In our case with far smaller grains, intergranular cracking was observed [12].

Metallurgical history affects the microstructure and in turn, will influence the fracture toughness. For example, K_{Ic} reported by Fields *et al.* [21] is as low as $1.7 \pm 0.3 \text{ MPa}\cdot\text{m}^{1/2}$ for Cu_3Sn and $1.4 \pm 0.3 \text{ MPa}\cdot\text{m}^{1/2}$ for Cu_6Sn_5 . They prepared the bulk specimens using powder metallurgy where microscopic pores are inevitable. Despite these differences, it is reasonable to summarize that Cu-Sn intermetallic compounds are brittle with fracture toughness no more than $6 \text{ MPa}\cdot\text{m}^{1/2}$. Among limited reports that are known to us, our test shows the best data consistence. The standard deviation in K_{Ic} is only around 6% in our study as compared to 15 - 38% for the rest.

4. Conclusion

We have described a controlled buckling test for thin film fracture toughness measurement where the thin film is deposited on a compliant substrate. When the substrate deforms by an elastic – linear work hardening constitution, the energy release rate is shown to be affected by the plastic deformation. Plastic deformation in the substrate promotes crack opening and thus increases the energy release rate. Such an effect is more pronounced with materials of low work hardenability. In practice, this means that the same film will crack more easily with more compliant substrate. Fracture toughness measurement in two types of Cu-Sn intermetallic thin films has been described. The results have been compared and discussed with other published data. Our test method show very consistent results.

References

- [1] K. N. Tu, J. W. Mayer, and L. C. Feldman, *Electronic Thin Film Science - for Electrical Engineers and Materials Scientists*, Macmillan, New York (1992)
- [2] C. Wohlrab, and M. Hofer, *Optical Engineering*, 34 (1995) 2712
- [3] W. F. Wu, and B. S. Chiou B, *Semiconductor Science and Technology*, 11 (2) (1996) 196
- [4] T. Minami, S. Ida, T. Miyata, and Y. Minamino, *Thin Solid Films*, 445 (2003) 268
- [5] S. Veprek, S. Reiprich and S. Z. Li, *Applied Physics Letters*, 66 (1995) 2640
- [6] M. Ueda , M.M. Silva , C. Otani , H. Reuther , M. Yatsuzuka , C.M. Lepienski , L.A. Berni, *Surface & Coating Technology*, 169 –170 (2003) 408
- [7] R. J. Narayan, P. N. Kumta, C. Sfeir, D.-H. Lee, D. Olton, and D. Choi, *JOM*, 56 (10) (2004) 38
- [8] B. Cotterell and Z. Chen, *International Journal of Fracture*, 104 (2000) 169
- [9] Z. Chen, B. Cotterell, W. Wang, E. Guenther and S. J. Chua, *Thin Solid Films*, 394 (2001) 202
- [10] Z. Chen, B. Cotterell and W. Wang, *Engineering Fracture Mechanics*, 69 (2002) 597
- [11] Z. Chen, T. Cahyadi, M. Li, B. Balakrisnan and C. C. Chum, *Proceedings of the 53rd Electronic Component & Technology Conference*, 27-30 May 2003, New Orleans USA, IEEE (2003) 844
- [12] B. Balakrisnan, C. C. Chum, M. Li, Z. Chen and T. Cahyadi, *Journal of Electronic Materials*, 32 (2003) 166
- [13] S. J. Britvec, *The Stability of Elastic Systems*, Pergamon Press, New York (1973)
- [14] J. L. Beuth, Jr, *Cracking of Thin Bonded Films in Residual Tension*, *International Journal of Solids and Structures*, 29 (1992) 1657
- [15] J. W. Hutchinson, *Mechanics of Thin Films and Multilayers*, Technical University of Denmark, 1996
- [16] J. W. Hutchinson, and Z. Suo, *Advances in Applied Mechanics*, 29 (1992) 63
- [17] J. H. Liu, A. G. Atkins, and A. J. Pretlove, *Journal of Mechanical Engineering Science*, 209 (2) (1995) 87
- [18] J. L. Beuth, and N. W. Klingbeil, *Journal of the Mechanics and Physics of Solids*, 44 (1996) 1411
- [19] J. H. Westbrook and R.L. Fleischer, eds., *Structural Applications of Intermetallic Compounds*, Wiley, New York (2000).

- [20] G. Ghosh, *Journal of Materials Research*, 19 (2004) 1493
- [21] R. J. Fields, S. R. Low III, and G. K. Lucey, Jr., in *The Metal Science of Joining*, edited by M. J. Cieslak, J. H. Perepezko, S. Kang, and M. E. Glicksman, TMS, Warrendale PA (1992) 165-173

List of Table

Table 1 Material properties and thickness of the polymer substrates and the intermetallic thin films.

List of Figures

- Figure 1 Schematics of a controlled buckling test. (a) Specimens with simple support (free) ends, (b) specimens with clamped (built-in) ends. The film is always placed on the tension (top) side of the plate.
- Figure 2 Controlled buckling test fixture operated manually under an optical microscope. Film cracking can be directly monitored during the experiment.
- Figure 3 $g\left(\alpha, \beta, \frac{\sigma}{\sigma_y}, \lambda\right)$ versus α for different values of (σ / σ_y) with $\beta = 0$. (a) $\lambda = 0.001$; (b) $\lambda = 0.05$.
- Figure 4 Effect of (σ / σ_y) on $g\left(\alpha, \beta, \frac{\sigma}{\sigma_y}, \lambda\right)$ at different λ 's with fixed $\alpha = 0.95$.
- Figure 5 SEM image of channelling cracks of a Cu-Sn intermetallic thin film.

Materials	E (GPa)	ν	h (μm)	G_{Ic} (J/m^2)	K_{Ic} ($\text{MPa}\cdot\text{m}^{1/2}$)
Ultem	2.6	0.36	175	/	/
Polycarbonate	2.3	0.36	500	/	/
Cu_3Sn	110	0.32	0.800	65.5 ± 8.0	2.83 ± 0.16
Cu_6Sn_5	90	0.32	0.800	55.9 ± 7.3	2.63 ± 0.15

E – elasticity modulus; ν – Poisson’s ratio; h – thickness; G_{Ic} – critical energy release rate;
 K_{Ic} – critical stress intensity factor

Table 1



(a)



(b)

Figure 1

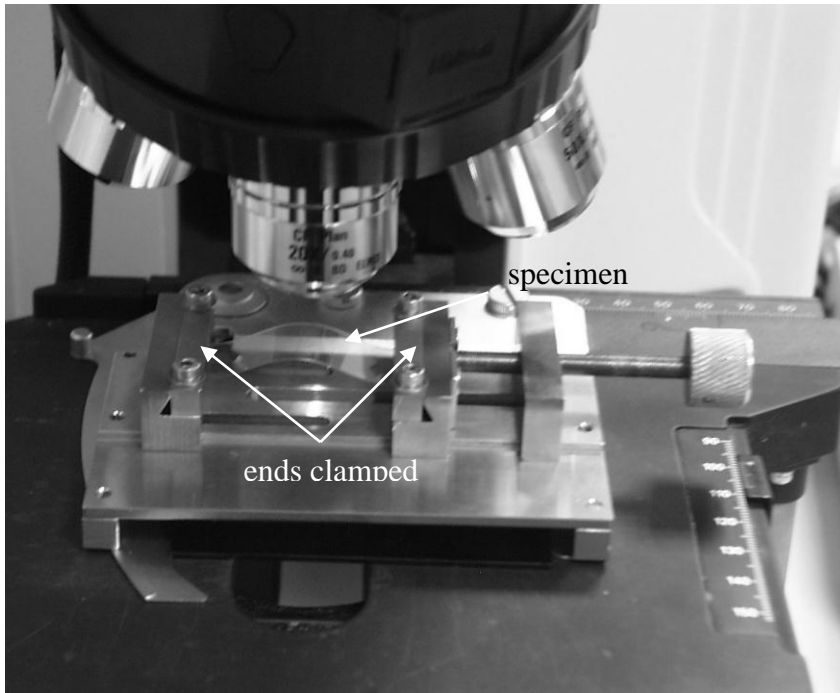
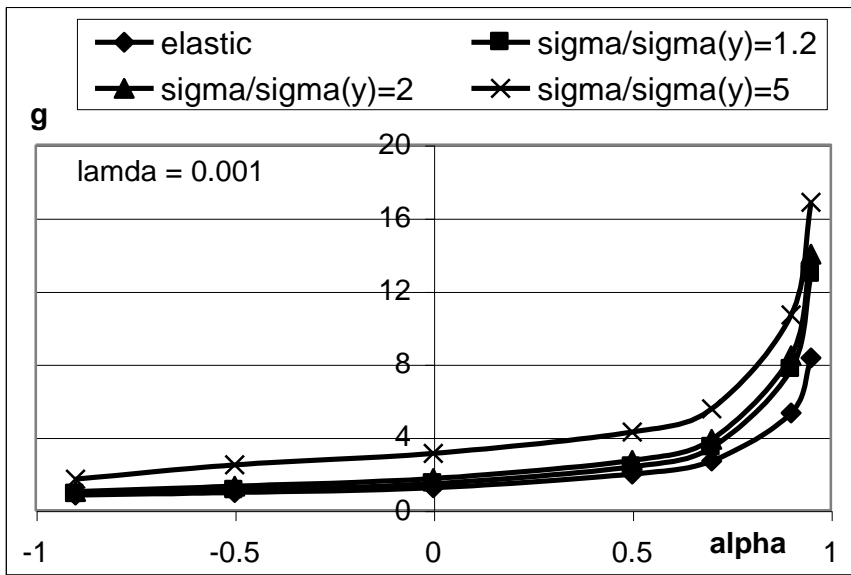
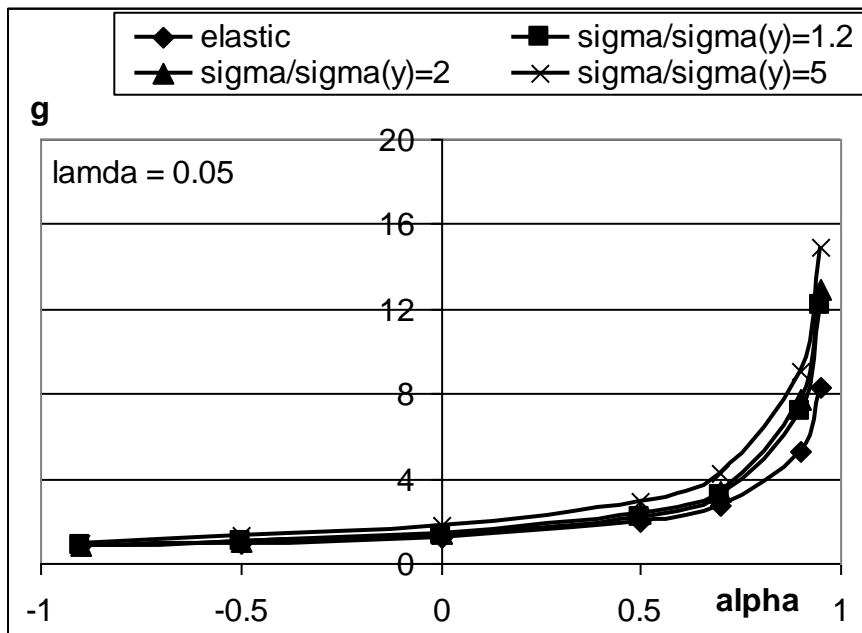


Figure 2



(a)



(b)

Figure 3

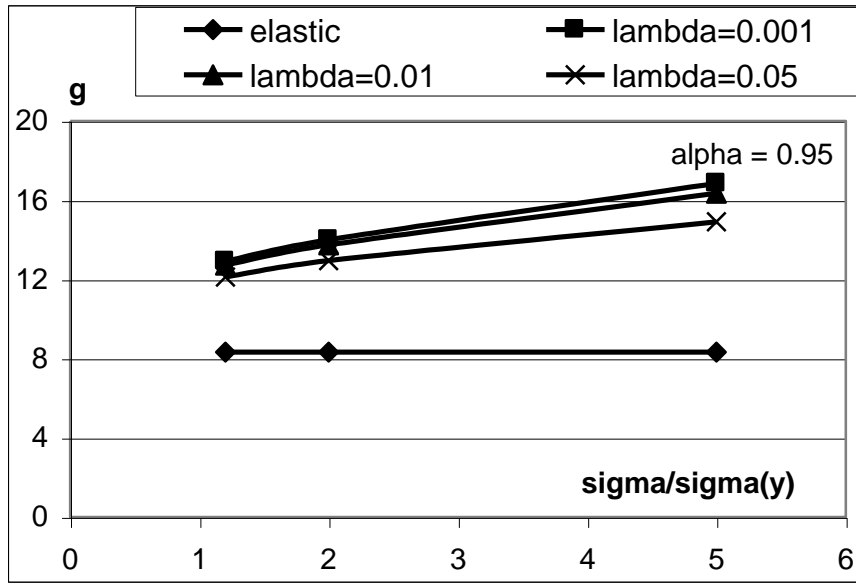


Figure 4

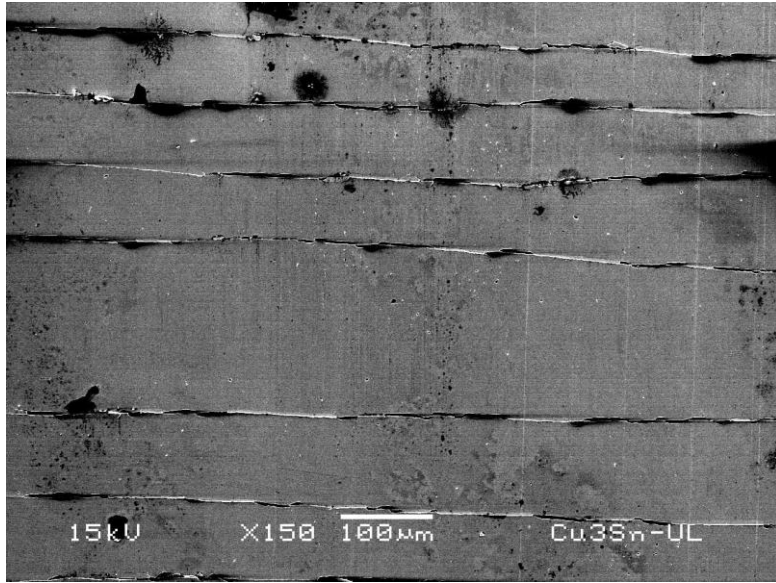


Figure 5